

Self-illuminating quantum dot conjugates for
in vivo imagingMin-Kyung So^{1,4}, Chenjie Xu^{1,4}, Andreas M Loening^{1,2}, Sanjiv S Gambhir^{1,2} & Jianghong Rao^{1,3}

Fluorescent semiconductor quantum dots hold great potential for molecular imaging *in vivo*^{1–5}. However, the utility of existing quantum dots for *in vivo* imaging is limited because they require excitation from external illumination sources to fluoresce, which results in a strong autofluorescence background and a paucity of excitation light at nonsuperficial locations. Here we present quantum dot conjugates that luminesce by bioluminescence resonance energy transfer in the absence of external excitation. The conjugates are prepared by coupling carboxylate-presenting quantum dots to a mutant of the bioluminescent protein *Renilla reniformis* luciferase. We show that the conjugates emit long-wavelength (from red to near-infrared) bioluminescent light in cells and in animals, even in deep tissues, and are suitable for multiplexed *in vivo* imaging. Compared with existing quantum dots, self-illuminating quantum dot conjugates have greatly enhanced sensitivity in small animal imaging, with an *in vivo* signal-to-background ratio of $> 10^3$ for 5 pmol of conjugate.

The unique optical properties of quantum dots, such as high quantum yields, large molar extinction coefficients, size-dependent tunable emission and high photostability^{6–10}, make them appealing as fluorescent probes for biological imaging^{5,11–14}. However, imaging quantum dots *in vivo* is challenging owing to the requirement for external illumination, which produces strong background autofluorescence from ubiquitous endogenous chromophores such as collagens, porphyrins and flavins¹⁵. In addition, because of absorption and scattering of optical photons in tissues, little light is available for quantum dot excitation at nonsuperficial locations¹⁶. An ideal quantum dot would emit light with no requirement for external excitation. Here we report a design for such a quantum dot, based on the principle of bioluminescence resonance energy transfer (BRET) (Fig. 1a).

BRET is a naturally occurring phenomenon whereby a light-emitting protein (the donor, such as *R. reniformis* luciferase) non-radiatively transfers energy to a fluorescent protein (the acceptor, such as green fluorescent protein) in close proximity^{17–19}. BRET is analogous to fluorescence resonance energy transfer (FRET), but the donor energy comes from a chemical reaction catalyzed by the donor enzyme (such as *R. reniformis* luciferase-mediated oxidation of its substrate coelenterazine) rather than from absorption of excitation photons. FRET has been shown to occur between quantum

dot donors and organic dye acceptors^{20,21}, but it has been argued that quantum dots cannot be FRET acceptors for organic fluorophores because of the long exciton lifetime of the quantum dot acceptor compared with that of the dye donor and substantial direct excitation of quantum dots²². Thus, before the present study, it was unclear whether quantum dots could replace fluorescent proteins as the BRET acceptor.

Bioluminescence *in vivo* imaging has extremely high sensitivity^{23,24}, and generally uses firefly luciferase²⁵ (maximal emission at ~ 560 nm) or *R. reniformis* luciferase²⁶ (maximal emission at 480 nm) as the reporter. To construct bioluminescent quantum dot conjugates, we chose *R. reniformis* luciferase because quantum dots absorb blue wavelengths more efficiently than longer-wavelength light (Fig. 1b). We recently developed an eight-mutation variant of *R. reniformis* luciferase (designated Luc8) that is more stable in serum and has improved catalytic efficiency compared with the wild-type protein (A.M.L., T.D. Fenn, A.M. Wu, & S.S.G., unpublished data). Luc8 emitted blue light with a peak at 480 nm upon addition of its substrate coelenterazine (Fig. 1b). We conjugated Luc8 to polymer-coated CdSe/ZnS core-shell quantum dot (QD) 655 (fluorescence emission at 655 nm) through coupling of the amino groups on Luc8 to carboxylates presented on the quantum dot. Gel electrophoresis analysis revealed a band with altered mobility, confirming successful conjugation (Fig. 1c). The hydrodynamic diameter of QD655-Luc8, measured by quasi-elastic light scattering, was ~ 2 nm larger than that of QD655. Each QD655-Luc8 conjugate was estimated to contain, on average, six copies of Luc8.

We examined the bioluminescence emission of QD655-Luc8 upon addition of coelenterazine (Fig. 1d). In addition to the emission of Luc8 at 480 nm, a strong new emission peak at 655 nm was detected, indicating that BRET occurred in the conjugate. The BRET ratio, determined by dividing the acceptor emission by the donor emission, was 1.29 (corresponding to an efficiency of 56%). For one mole of QD655-Luc8, the maximal blue photon emission (from Luc8) was 3.0×10^{22} photons/s, and the maximal red photon emission (from QD655) was 3.6×10^{22} photons/s.

The BRET ratio was dependent on the distance between Luc8 and QD655. When the mean distance between Luc8 and QD655 was increased by ~ 2 – 3 nm, the BRET ratio dropped to ~ 0.37 (Supplementary Fig. 1 and Supplementary Notes online). When the ratio of QD655 to Luc8 in the coupling reaction was varied to produce

¹Molecular Imaging Program at Stanford, Department of Radiology & Bio-X Program, ²Department of Bioengineering, ³Biophysics Program, Stanford University, 1201 Welch Road, Stanford, California 94305-5484, USA. ⁴These authors contributed equally to this work. Correspondence should be addressed to J.R. (jrao@stanford.edu).

Received 8 September 2005; accepted 12 January 2006; published online 26 February 2006; doi:10.1038/nbt1188

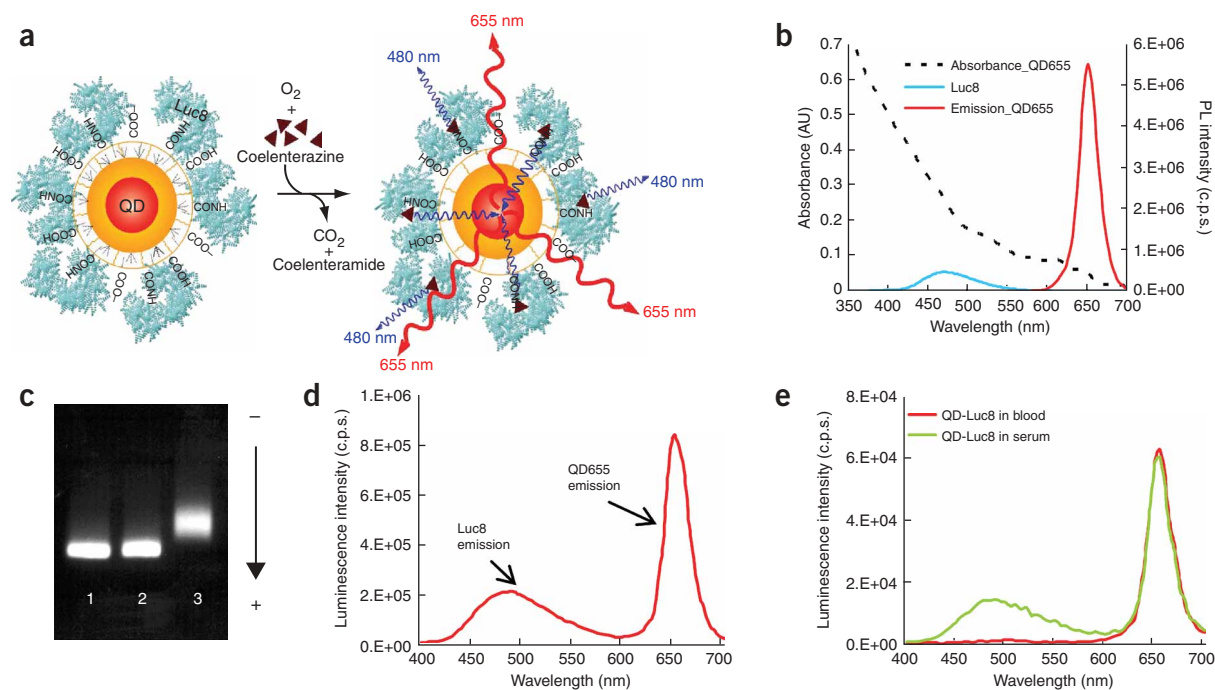


Figure 1 Design and spectroscopic characterization of bioluminescent quantum dot conjugates based on BRET. **(a)** A schematic of a quantum dot that is covalently coupled to a BRET donor, Luc8. The bioluminescence energy of Luc8-catalyzed oxidation of coelenterazine is transferred to the quantum dots, resulting in quantum dot emission. **(b)** Absorption and emission spectra of QD655 ($\lambda_{\text{ex}} = 480 \text{ nm}$), and spectrum of the bioluminescent light emitted in the oxidation of coelenterazine catalyzed by Luc8. **(c)** Gel electrophoresis analysis of the conjugation of Luc8 to QD655: (1) unconjugated QD655, (2) the mixture of QD655 and the coupling reagent EDC and (3) purified QD655-Luc8 conjugates. **(d)** Bioluminescence emission spectrum of QD655-Luc8 in borate buffer. **(e)** Bioluminescence emission spectrum of QD655-Luc8 in mouse serum and in mouse whole blood.

conjugates with varying numbers of Luc8, the BRET ratios of the conjugates were surprisingly similar, ranging from 1.10 to 1.46, although the intensity of both Luc8 and quantum dot emissions varied by >100 -fold (**Supplementary Fig. 2** and **Supplementary Notes** online). This is different from FRET examples, where the FRET efficiency improves as the number of FRET acceptors per quantum dot increases²⁰.

With the aim of assessing whether BRET emission could be detected *in vivo*, we first examined emission of QD655-Luc8 in mouse serum and whole blood. Whereas Luc8 emission of QD655-Luc8 nearly disappeared in whole blood because of absorption by hemoglobin, the BRET emission of QD655-Luc8 was barely affected (**Fig. 1e**). Next, we subcutaneously injected a solution of QD655-Luc8 (5 pmol) into the left shoulder of a nude mouse (site I in **Fig. 2a**). As a control, a solution of Luc8 (30 pmol) was similarly injected into the right shoulder of the same mouse (site II in **Fig. 2a**). The mouse was imaged sequentially after tail-vein injection of coelenterazine, both without any filter (to collect the emission from Luc8 and QD655; **Fig. 2a**) and with an emission filter (575–650 nm, to collect the QD655 emission; **Fig. 2b**). Images collected without any filter showed strong signals from both injection sites (**Fig. 2a**). The total photon fluxes in each site were similar, indicating that the activity of Luc8 in each site was approximately the same. With the filter, there was still a strong signal from site I (QD655-Luc8, **Fig. 2b**), which was 60% of the intensity collected without the filter. However, the Luc8 signal from site II with the filter (site II, **Fig. 2b**) was just 25% of that collected without the filter. Using a filter (650–660 nm) for more specific collection of the BRET emission, the signal detected from site II was even lower, whereas site I still emitted a strong signal (**Supplementary**

Fig. 3 online). These results indicate that BRET between Luc8 and quantum dots can occur in animals at superficial depths.

We next studied BRET emission in deeper tissues. A solution of QD655-Luc8 (5 pmol) was injected intramuscularly at a depth of $\sim 3 \text{ mm}$ (site III in **Fig. 2a**), and a solution of Luc8 (30 pmol) was similarly injected into the same nude mouse (site IV in **Fig. 2a**). In contrast to the subcutaneous injections (sites I and II in **Fig. 2a**), the emission of intramuscularly injected Luc8, even without any filter, was much weaker than that of QD655-Luc8 (IV versus III in **Fig. 2a**): the total detected photons from site IV was only 26% of that from site III. With the filter (575–650 nm), there was little detectable signal from

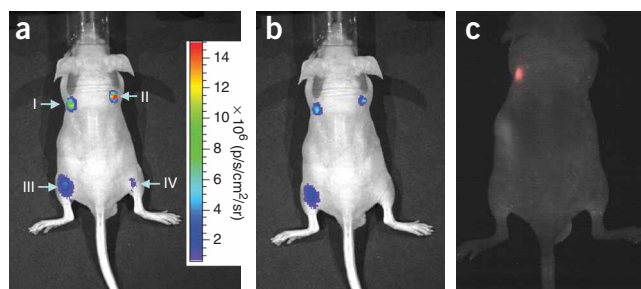


Figure 2 Bioluminescence and fluorescence imaging of QD655-Luc8 and Luc8 injected subcutaneously (I and II) and intramuscularly (III and IV) at indicated sites in a mouse (I and III, QD655-Luc8, 5 pmol; II and IV, Luc8, 30 pmol). **(a)** Open without filters. **(b)** With 575- to 650-nm filter. **(c)** Fluorescence imaging of the same mouse injected with indicated solutions in **a** (excitation filter, 503–555 nm).

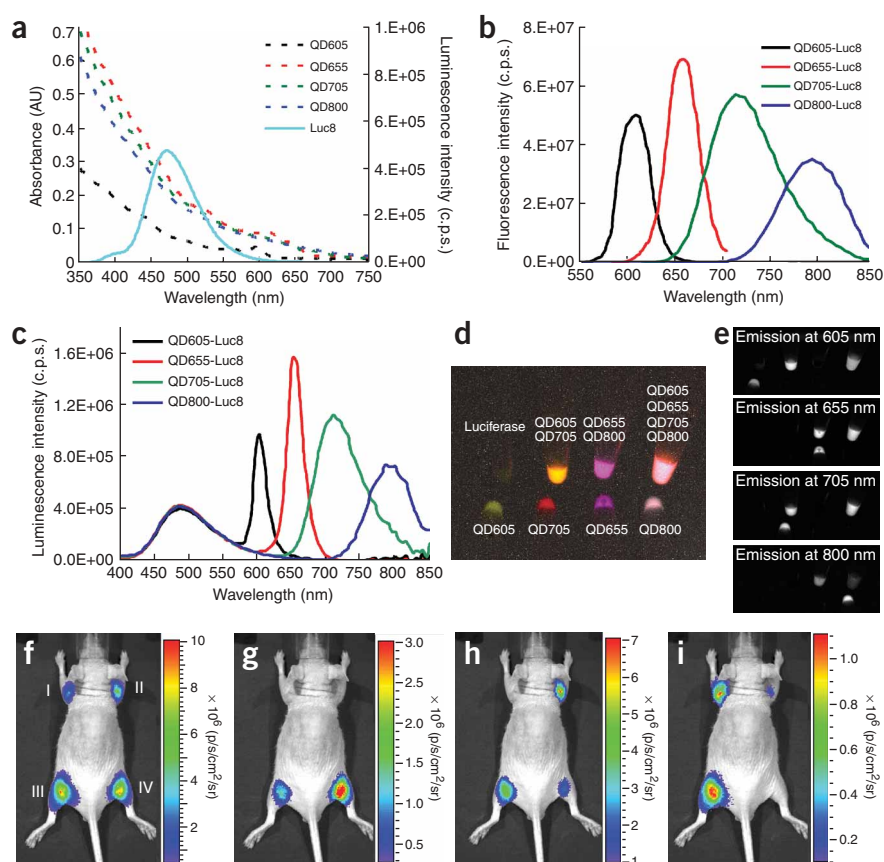


Figure 3 Multiplexed imaging of conjugates QD605-Luc8, QD655-Luc8, QD705-Luc8 and QD800-Luc8 *in vitro* and in mice. **(a)** Overlap of the bioluminescence emission of Luc8 with the absorption spectra of QD605, QD655, QD705 and QD800. **(b)** Fluorescence ($\lambda_{ex} = 480$ nm) emission spectra of indicated conjugates. **(c)** Bioluminescence emission spectra of indicated conjugates. **(d)** *In vitro* bioluminescence spectral imaging of solutions containing indicated conjugates. Image was collected for emission from 580 to 850 nm. The different emissions are shown in pseudo colors. Sample at top left contained only Luc8, which showed no detectable long-wavelength (580–850 nm) emission. **(e)** *In vitro* bioluminescence spectral imaging of the same samples as in **d**, but images were collected at the indicated emission wavelengths. **(f–i)** Multiplexed *in vivo* bioluminescence imaging of the following conjugates intramuscularly injected at the indicated sites: (I) QD800-Luc8, 15 pmol; (II) QD705-Luc8, 15 pmol; (III) a mixture of QD665-Luc8, QD705-Luc8 and QD800-Luc8; and (IV) QD655-Luc8, 5 pmol. Images were collected with the following emission filters: **(f)** without any filter, **(g)** with 575- to 650-nm filter, **(h)** with x-Cy5.5 filter (680–720 nm) and **(i)** with ICG filter (810–875 nm). The acquisition time for each image was 30 s.

shows the fluorescence emission spectrum and **Figure 3c** the bioluminescence spectrum of each quantum dot conjugate. Clearly, BRET occurs in each conjugate. The BRET

ratios are estimated as 0.70 for QD605-Luc8, 1.20 for QD655-Luc8, 2.30 for QD705-Luc8 and 1.32 for QD800-Luc8. This trend correlates well with the excitability of each quantum dot (**Supplementary Table 1** online). For example, QD705 and QD800 have the same extinction coefficient ($1,700,000 \text{ M}^{-1}\text{cm}^{-1}$ at 550 nm), but the quantum yield of QD705 is 80% and only 43% for QD800, hence the BRET ratio of QD800-Luc8 is just about half that of QD705-Luc8.

The spectrally distinct emissions of the four conjugates make multiplexed bioluminescence imaging feasible. We examined this possibility by first imaging solutions containing QD605-Luc8, QD655-Luc8, QD705-Luc8, QD800-Luc8 and a mixture of all four *in vitro* (**Fig. 3d,e**). Using bioluminescence spectral imaging (analogous to fluorescence spectral imaging but without excitation light), we could selectively distinguish the bioluminescence emission of each conjugate from the others whether it was alone or in a mixture.

We intramuscularly injected QD655-Luc8, QD705-Luc8, QD800-Luc8 and a mixture of the three conjugates at four different sites on a nude mouse for *in vivo* multiplexed bioluminescence imaging. The total emission (from Luc8 and BRET) was collected without any filter (**Fig. 3f**), and the BRET emission was collected with appropriate filters, for example, the x-Cy5.5 filter for QD705-Luc8 and the ICG filter for QD800-Luc8 (**Fig. 3g–i**). Similarly to the *in vitro* imaging results, all conjugates showed Luc8 emission, and each BRET emission was readily distinguished with appropriate filters, although there was a small degree of signal cross-talk due to overlap of the emission spectra of QD655-Luc8 and QD705-Luc8, and of QD705-Luc8 and QD800-Luc8 (**Fig. 3b**). This small degree of signal cross-talk could be reduced with filters better designed for quantum dots.

the injected Luc8 but a strong signal from QD655-Luc8 (**Fig. 2b**). The bioluminescence intensity of the injected QD655-Luc8 imaged with the filter was 75% of that without the filter. The increased ratio of detected QD655 emission versus Luc8 emission is due to more substantial absorption and scattering of the shorter-wavelength Luc8 emission in tissues. Therefore, in deep tissues, the longer-wavelength BRET emission of QD655-Luc8 is more readily detected than the shorter-wavelength emission from Luc8.

The same mouse was examined with fluorescence spectral imaging for quantum dot fluorescence emission. A strong signal was observed from subcutaneously injected QD655-Luc8, but intramuscularly injected QD655-Luc8 emitted only a weak signal (**Fig. 2c**), demonstrating the advantages of bioluminescence detection of signals from deep tissues with bioluminescent quantum dot conjugates. Fluorescence imaging of quantum dots requires external light to pass into tissues for excitation. Because of substantial absorption and scattering of the short-wavelength excitation photons in tissues, light emission by BRET is more efficient than by external illumination (**Supplementary Notes** online). In addition, by eliminating the need for excitation light, the preferential illumination of fluorophores near the surface that occurs with traditional reflectance fluorescence imaging systems is removed, and the issue of background autofluorescence is completely avoided.

A longstanding goal of bioluminescence *in vivo* imaging is to have several probes with distinct long-wavelength emissions for multiple target imaging. Because quantum dots have similar absorption spectra and absorb blue light efficiently, Luc8 can also serve as the BRET donor for quantum dots other than QD655 (**Fig. 3a**). We prepared conjugates QD705-Luc8, QD800-Luc8 and QD605-Luc8. **Figure 3b**

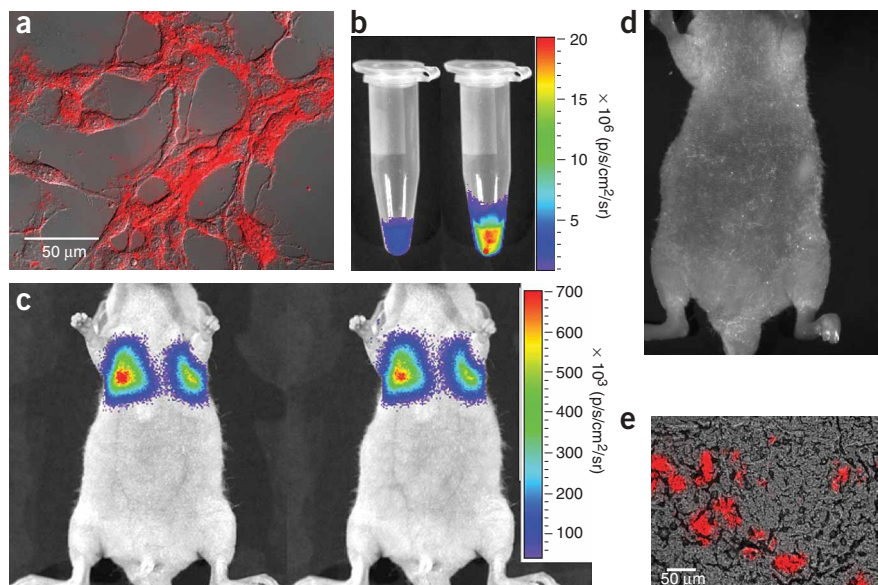


Figure 4 Imaging C6 glioma cells labeled with QD655-Luc8-R9 *in vitro* and in mice. **(a)** Overlay of fluorescence and differential interference contrast (DIC) images of QD655-Luc8-R9-labeled C6 glioma cells. Fluorescence image was collected with the following filter set (Chroma Technology): excitation, 420/40; emission, D660/40; dichroic, 475DCXR. Scale bar, 50 μm . **(b)** Representative bioluminescence images of labeled cells acquired with a filter (575–650 nm) (left) and without any filter (right). **(c)** Representative bioluminescence images of a nude mouse injected via tail vein with labeled cells, acquired with a filter (575–650 nm) (left) and without any filter (right). **(d)** Fluorescence image of the same mouse in **c** (excitation filter, 503–555 nm). **(e)** Overlay of fluorescence and DIC images of a lung slice of the same mouse imaged in **c** and **d** shows the accumulation of quantum dot conjugates in the lungs; the same filter set as in **a** was used. Scale bar, 50 μm .

Finally, we evaluated whether our BRET conjugates could be used to label cells and to monitor labeled cells in animals. QD655-Luc8 was conjugated with a polycationic peptide (arginine 9-mer) to improve the cell uptake efficiency (QD655-Luc8-R9)³. The BRET ratio of QD655-Luc8-R9 was comparable to that of QD655-Luc8, indicating that conjugation of R9 had little impact on BRET. Cells incubated with QD655-Luc8-R9 for 1 h at 37 °C displayed bright QD655 fluorescent signals (Fig. 4a). These cells were collected for bioluminescence imaging in the absence (right tube in Fig. 4b) and presence of a BRET filter (575–650 nm) (left tube in Fig. 4b). The ratio of total emission from the left tube to that from the right tube was ~ 0.20 , which is close to the calculated value, 0.18, based on the *in vitro* emission spectrum of QD655-Luc8 (Fig. 1d). These results confirmed that QD655-Luc8-R9 conjugates were functional and produced BRET emission after being taken up into cells.

The QD655-Luc8-R9-labeled cells ($\sim 2 \times 10^6$) were injected through the tail vein into a nude mouse to examine whether BRET signals from the labeled cells could be detected. The total intensity of the signals is approximately the same in the lungs of the mouse, whether collected with the BRET filter (Fig. 4c, left) or without (Fig. 4c, right), suggesting that Luc8 emission was largely scattered and absorbed in deep tissues. No bioluminescence emission was produced in a control mouse injected with unlabeled cells. For comparison, we performed fluorescence spectral imaging of the same mouse: no detectable quantum dot fluorescence emission was seen arising from the lungs (Fig. 4d). Epifluorescence microscopic examination of slices of lung confirmed the presence of QD655-Luc8-R9 (Fig. 4e).

We have reported here self-illuminating quantum dot conjugates designed by mimicking a natural BRET system, with a mutant of

R. reniformis luciferase as the energy donor and quantum dots as the acceptor, and have demonstrated that BRET emission can be imaged in cells and small animals. These quantum dot conjugates offer several useful features: (i) they are compatible with both bioluminescence and fluorescence imaging, and the ability to image them without external excitation (bioluminescently) results in greatly enhanced sensitivity in small-animal imaging; (ii) their long-wavelength (from red to near-infrared) bioluminescence emissions are readily detectable even in deep tissues; (iii) their distinct BRET emission spectra allow *in vivo* multiplexed bioluminescence imaging of multiple targets. Bioluminescent quantum dot probes should open many new avenues for molecular imaging, including highly sensitive *in vitro* assays, *in vivo* cell trafficking studies, multiplexed imaging, and the design of biosensors whose BRET emission is modulated by specific biological interactions.

METHODS

Materials. Quantum dots were from Quantum Dot Corp. QD605 and QD655 have typical CdSe/ZnS core-shell structures, and QD705 and QD800 are made of CdTe cores with ZnS coatings. The organic coating chemistry has been previously described in the literature¹³, and the final coated quantum dots are endowed with carboxylate groups. The quantum yields of each quantum dot determined in 50 mM borate buffer (pH 9) are 65% (QD605), 83% (QD655), 80% (QD705) and 43% (QD800). The hydrodynamic diameters of all quantum dots and conjugates were measured by Malvern Instruments Ltd. with a Zetasizer Nano ZS. The coupling reagent 1-ethyl-3-(3-dimethylamino-propyl)carbodiimide hydrochloride (EDC) was from Fluka. Coelenterazine, the substrate for Luc8, was from Prolume. All other chemicals and solvents were from Sigma-Aldrich. Nude mice (4–6 weeks old) were from Charles River Breeding Laboratories. Fluorescence and bioluminescence emission spectra were collected with a Fluoro Max-3 (Jobin Yvon Inc.); in the case of bioluminescence, the excitation light was blocked, and emission spectra were corrected with a correction file provided by the company. Bioluminescence emission spectra collected with the spectrofluorometer were further corrected for the Luc8 kinetics over the course of data acquisition (typically ~ 20 s). Enzymatic activity of Luc8 was measured with a 20/20⁺ Luminometer (Turner Biosystems, Inc.). Animal use protocols were reviewed and approved by the Institutional Animal Care Use Committee of Stanford University.

Preparation of QD-Luc8 conjugates. To a mixture of 8.2 pmol of quantum dots and 164 pmol of Luc8 (20 equivalents) in 200 μl borate buffer (pH 7.4), we added 32.8 nmol of EDC (4,000 equivalents). Borate buffer was chosen to minimize quantum dot aggregation during the coupling. The mixture was incubated for 1 h, and the uncoupled free Luc8 and excess EDC were removed by three washes using a 100 K NanoSep filter (Pall Corporation) by centrifugation at 2655g for 3 min at 4 °C. The final complex was kept in borate buffer at 4 °C.

Gel electrophoresis. We ran 1.0 pmol of QD655-Luc8 conjugates, QD655 and the reaction mixture of QD655 and EDC, with 6 \times loading dye on a 0.5% agarose gel at 100 V in TAE buffer (0.5 \times).

Cell labeling with QD-Luc8-R9. We activated 8.2 pmol of QD655-Luc8 by 8.2 nmol of EDC (1,000 equivalents) for 5 min. We then added 1.64 nmol of peptide R9 (200 equivalents), and the mixture was incubated for 30 min. The

conjugated product was purified using a 100-K NanoSep filter as before. C6 rat glioma cells were cultured in Dulbecco's Modified Eagle Medium supplemented with 10% FBS (Gibco) and 1% antibiotic-antimycotic mixture (Gibco). Before incubation with quantum dot conjugates, culture media were replaced by HBSS. After incubation with QD-Luc8-R9 (1 ml, 10 nM) at 37 °C for 1 h, cells were washed with HBSS three times and imaged with an inverted fluorescence microscope (Axiovert 200M, Zeiss). The following filter set (Chroma Technology Corporation) was used for QD655 analysis: excitation, 420/40; emission, D660/40; dichroic, 475DCXR. Acquisition time: 50 ms, and 40× magnification. For bioluminescence imaging of labeled cells, cells were collected by trypsinization or cell scrapers, and suspended in 50 µl of HBSS. After addition of 2 µg of coelenterazine, cells were imaged immediately with an IVIS 200 bioluminescence imaging system (Xenogen) with and without filter (30 s for each acquisition).

In vivo bioluminescence imaging. Quantum dot conjugates (or labeled cells) were injected either subcutaneously, intramuscularly or through the tail vein into nude mice. Mice were subsequently anesthetized with isoflurane, and transferred into the light-tight chamber of an IVIS 200 imager. After 10 min, coelenterazine (10 µg/mouse in 10 µl methanol and 90 µl phosphate buffer) was injected intravenously. Images were acquired with and without filters. Each acquisition took 30 s (for injected quantum dot conjugates) or 2 min (for labeled cells). To correct for the relatively fast *in vivo* pharmacokinetics of coelenterazine, we acquired the images sequentially: (i) with filter (30 s); (ii) without filter (30 s); (iii) without filter (30 s); (iv) with filter (30 s). The emission with filter was calculated from the average of 1 and 4, and the emission without filter was the average of 2 and 3.

In vivo fluorescence imaging. Wavelength-resolved spectral imaging was carried out using a spectral imaging system (Maestro In-Vivo Imaging System from Cambridge Research & Instrumentation). The excitation filter was 503–555 nm. The tunable filter was automatically stepped in 10-nm increments from 580 to 900 nm with an exposure time of 49 ms for images captured at each wavelength. Animals were placed supine under isoflurane anesthesia in a light-tight chamber. Collected images were analyzed by the Maestro software, which uses spectral unmixing algorithms to separate autofluorescence from quantum dot signals. The *in vitro* multiplexed bioluminescence imaging of quantum dot conjugates was performed similarly with the Maestro system, but with the excitation light blocked and 5-s exposure time for each individual acquisition.

Histology. Nude mice were killed 1 h and 20 min after injection of quantum dot-labeled cells. Lungs were collected, washed with PBS, frozen in isopropanol with liquid nitrogen and stored at –80 °C. Frozen samples were sectioned by microtome at a thickness of 10 µm. Slides were analyzed under a Zeiss inverted fluorescence microscope with the same quantum dot filter set as described above (objective, 20×; acquisition time, 1 s).

Note: Supplementary information is available on the Nature Biotechnology website.

ACKNOWLEDGMENTS

This work was supported by the Burroughs Wellcome Fund (to J.R.), the Korea Research Foundation Grant M07-2004-000-10234-0 (to M.-K.S.), a Stanford Bio-X Graduate Fellowship (to A.M.L.), the National Institutes of Health grants 5R01CA82214-7 and P50 CA114747 (to S.S.G.), the National Cancer Institute Centers of Cancer Nanotechnology Excellence (CCNE) U54, and the National Cancer Institute's Small Animal Imaging Resource Program (SAIRP R24CA92862).

COMPETING INTERESTS STATEMENT

The authors declare competing financial interests (see the *Nature Biotechnology* website for details).

Published online at <http://www.nature.com/naturebiotechnology/>

Reprints and permissions information is available online at <http://npg.nature.com/reprintsandpermissions/>

1. Michalet, X. *et al.* Quantum dots for live cells, *in vivo* imaging, and diagnostics. *Science* **307**, 538–544 (2005).
2. Kim, S. *et al.* Near-infrared fluorescent type II quantum dots for sentinel lymph node mapping. *Nat. Biotechnol.* **22**, 93–97 (2004).
3. Gao, X., Cui, Y., Levenson, R.M., Chung, L.W.K. & Nie, S. *In vivo* cancer targeting and imaging with semiconductor quantum dots. *Nat. Biotechnol.* **22**, 969–976 (2004).
4. Jaiswal, J.K. & Simon, S.M. Potentials and pitfalls of fluorescent quantum dots for biological imaging. *Trends Cell Biol.* **14**, 497–504 (2004).
5. Medintz, I.L., Uyeda, H.T., Goldman, E.R. & Mattoussi, H. Quantum dot bioconjugates for imaging, labelling and sensing. *Nat. Mater.* **4**, 435–446 (2005).
6. Dabbousi, B.O. *et al.* (CdSe)ZnS core-shell quantum dots: Synthesis and characterization of a size series of highly luminescent nanocrystallites. *J. Phys. Chem. B* **101**, 9463–9475 (1997).
7. Leatherdale, C.A., Woo, W.K., Mikulec, F.V. & Bawendi, M.G. On the absorption cross section of CdSe nanocrystal quantum dots. *J. Phys. Chem. B* **106**, 7619–7622 (2002).
8. Bruchez, M., Moronne, M., Gin, P., Weiss, S. & Alivisatos, A.P. Semiconductor nanocrystals as fluorescent biological labels. *Science* **281**, 2013–2016 (1998).
9. Chan, W.C.W. & Nie, S. Quantum dot bioconjugates for ultrasensitive nonisotopic detection. *Science* **281**, 2016–2018 (1998).
10. Niemeyer, C.M. Nanoparticles, proteins, and nucleic acids: Biotechnology meets materials science. *Angew. Chem. Int. Edn. Engl.* **40**, 4128–4158 (2001).
11. Pinaud, F., King, D., Moore, H-P. & Weiss, S. Bioactivation and cell targeting of semiconductor CdSe/ZnS nanocrystals with phytochelatin-related peptides. *J. Am. Chem. Soc.* **126**, 6115–6123 (2004).
12. Mamedova, N.N., Kotov, N.A., Rogach, A.L. & Studer, J. Albumin-CdTe nanoparticle bioconjugates: preparation, structure, and interunit energy transfer with antenna effect. *Nano Lett.* **1**, 281–286 (2001).
13. Wu, X. *et al.* Immunofluorescent labeling of cancer marker Her2 and other cellular targets with semiconductor quantum dots. *Nat. Biotechnol.* **21**, 41–46 (2003).
14. Dubertret, B. *et al.* *In vivo* imaging of quantum dots encapsulated in phospholipid micelles. *Science* **298**, 1759–1762 (2002).
15. Troy, T., Jekic-McMullen, D., Sambucetti, L. & Rice, B. Quantitative comparison of the sensitivity of detection of fluorescent and bioluminescent reporters in animal models. *Mol. Imaging* **3**, 9–23 (2004).
16. Tuchin, V. *Tissue optics* (SPIE Press, Bellingham, Washington, 2000).
17. Ward, W.W. & Cormier, M.J. Energy transfer via protein-protein interaction in *Renilla* bioluminescence. *Photochem. Photobiol.* **27**, 389–396 (1978).
18. Wilson, T. & Hastings, J.W. Bioluminescence. *Annu. Rev. Cell Dev. Biol.* **14**, 197–230 (1998).
19. De, A. & Gambhir, S.S. Non-invasive imaging of protein-protein interactions from live cells and living subjects using bioluminescence resonance energy transfer. *FASEB J.* **19**, 2017–2019 (2005).
20. Medintz, I.L. *et al.* Self-assembled nanoscale biosensors based on quantum dot FRET donors. *Nat. Mater.* **2**, 630–638 (2003).
21. Medintz, I.L. *et al.* A fluorescence resonance energy transfer-derived structure of a quantum dot-protein bioconjugate nanoassembly. *Proc. Natl. Acad. Sci. USA* **101**, 9612–9617 (2004).
22. Clapp, A.R., Medintz, I.L., Fisher, B.R., Anderson, G.P. & Mattoussi, H. Can luminescent quantum dots be efficient energy acceptors with organic dye donors? *J. Am. Chem. Soc.* **127**, 1242–1250 (2005).
23. Massoud, T.F. & Gambhir, S.S. Molecular imaging in living subjects: seeing fundamental biological processes in a new light. *Genes Dev.* **17**, 545–580 (2003).
24. Contag, C.H. & Bachmann, M.H. Advances in *in vivo* bioluminescence imaging of gene expression. *Annu. Rev. Biomed. Eng.* **4**, 235–260 (2002).
25. Contag, P.R., Olomu, I.N., Stevenson, D.K. & Contag, C.H. Bioluminescent indicators in living mammals. *Nat. Med.* **4**, 245–247 (1998).
26. Bhaumik, S. & Gambhir, S.S. Optical imaging of *Renilla* luciferase reporter gene expression in living mice. *Proc. Natl. Acad. Sci. USA* **99**, 377–382 (2002).